Fast Convergent Green's Function in a Rectangular Enclosure

Amir Borji* and S.Safavi-Naeini

Department of ECE, University of Waterloo, Waterloo, Ontario, Canada N2L 3G1
Email: amir@maxwell.uwaterloo.ca, Fax: (519)746-3077

Abstract

Ewald summation technique has been proven to be a highly efficient method for rapid calculation of the potential Green's functions in rectangular cavities. It is known that in addition to potential Green's functions, curl of the vector potential Green's function is also needed when applying the mixed potential integral equation method to dielectric objects. In this paper the Ewald sum technique is applied for rapid calculation of these components of the dyadic Green's functions. Several numerical implementation issues including the extraction of singularity when using the Ewald summation method are also addressed for the first time, leading to further enhancement in computational speed, accuracy, and numerical stability.

I. Introduction

The integral equation technique with method of moments is a potentially efficient method for EM analysis of shielded dielectric and metallic objects. In particular, mixed potential surface integral equation approach is known to be more advantageous but the slow convergence of the relevant Green's functions inside rectangular enclosure is the major obstacle in applying this method for shielded objects. The Ewald summation technique has proven to be a very effective tool for rapid calculation of potential Green's functions in periodic structures as well as cavities and waveguides [1,2]. In this paper the Ewald method is applied to calculate the gradient of the components of vector potential Green's functions inside a rectangular cavity. These components of the dyadic Green's functions are needed when applying the MPIE technique to shielded dielectric objects. Extraction of the singular terms in the Green's functions and expressions for the residue terms are also reported. It is also shown that using a numerical quadrature instead of calculating the complex error function further enhances the computational speed. Finally, a substantial loss of accuracy at very high frequencies is observed and a remedy for this problem is also presented.

II. Theory

A. Vector Potential Function and Its Curl

Mathematical derivations related to the Ewald method for potential Green's functions are presented in the literature [1,2] and here we use the final expressions in [2]. *Note that throughout this paper, all physical dimensions are normalized to the free-space wavelength, λ_o.* After applying the Ewald sum technique, *every component of the scalar or vector potential Green's functions in a rectangular cavity is cast into two exponentially convergent series* and can be represented in the following general form [2]:

$$G_1 = \frac{1}{4abc\,\lambda_o\pi^2} \sum_{m=0}^{+\infty} \sum_{n=0}^{+\infty} \sum_{p=0}^{+\infty} \frac{\epsilon_m\epsilon_n\epsilon_p}{\beta_{mnp}^2 - \epsilon_r}\, e^{-\frac{\pi^2(\beta_{mnp}^2 - \epsilon_r)}{E^2}} g_{mnp}(x,y,z)g_{mnp}(x',y',z') \tag{1a}$$

$$G_2 = \frac{1}{4\pi\lambda_o} \sum_{m=-\infty}^{+\infty} \sum_{n=-\infty}^{+\infty} \sum_{p=-\infty}^{+\infty} \sum_{i=0}^{7} A_i f(R_{i,mnp}) \tag{1b}$$

$$\beta_{mnp}^2 = \left(\frac{m}{2a}\right)^2 + \left(\frac{n}{2b}\right)^2 + \left(\frac{p}{2c}\right)^2 \quad , \quad R_{i,mnp} = \sqrt{(X_i+2ma)^2 + (Y_i+2nb)^2 + (Z_i+2pc)^2}$$

$G = G_1 + G_2$ is the component of the Green's function. $f(R)$ is given by:

$$f(R) = \frac{\Re\left[e^{-j2\pi\sqrt{\epsilon_r}\,R}\,erfc\left(RE - j\frac{\pi\sqrt{\epsilon_r}}{E}\right)\right]}{R} \tag{2}$$

E is the splitting parameter and *we replace $\lambda_o E$ by E throughout this article*. The only differences among the 8 different components of the potential functions are $g_{mnp}(x,y,z)$ and coefficients A_i. g_{mnp} is a modal function and always appears as a product of sine and cosine terms and A_i is $+1$ or -1 representing the sign of the source and its images. As an example, g_{mnp} for G_A^{xx} component is the following:

$$g_{mnp}(x,y,z) = \cos\frac{m\pi x}{a}\sin\frac{n\pi y}{b}\sin\frac{p\pi z}{c} \tag{3}$$

A_i coefficients for G_A^{xx} are given in [2] and X_i, Y_i, and Z_i also appear in [2].

The electric and magnetic vector potentials inside the cavity are both diagonal dyadics. To calculate the electric field due to a magnetic current or the magnetic field due to an electric current, the curl of the

vector potential Green's functions are needed. Additionally, $\nabla \times \bar{G}_A \cdot \vec{J}$ can be expanded in the following form:

$$\nabla \times \bar{G}_A \cdot \vec{J} = \nabla G_A^{xx} \times J_x \hat{x} + \nabla G_A^{yy} \times J_y \hat{y} + \nabla G_A^{zz} \times J_z \hat{z} \qquad (4)$$

therefore in the solution of MPIE via MoM, one needs to calculate the partial derivatives of different components of the potential Green's dyads. This can be done by taking the gradient of Eq. 1 with negligible effect on its convergence:

$$\nabla G_1 = \frac{1}{4abc\,\lambda_0^2\pi^2} \sum_{m=0}^{+\infty} \sum_{n=0}^{+\infty} \sum_{p=0}^{+\infty} \frac{\epsilon_m \epsilon_n \epsilon_p}{\beta_{mnp}^2 - \epsilon_r} e^{-\frac{\pi^2(\beta_{mnp}^2 - \epsilon_r)}{E^2}} \nabla g_{mnp}(x,y,z) g_{mnp}(x',y',z') \qquad (5a)$$

$$\nabla G_2 = \frac{1}{4\pi\lambda_0^2} \sum_{m=-\infty}^{+\infty} \sum_{n=-\infty}^{+\infty} \sum_{p=-\infty}^{+\infty} \sum_{i=0}^{7} A_i \frac{d}{dR} f(R_{i,mnp}) \nabla R_{i,mnp} \qquad (5b)$$

As an example $\nabla g_{mnp}(x,y,z)$ for G_A^{xx} is equal to:

$$\nabla g_{mnp} = -\frac{m\pi}{a} \sin\frac{m\pi x}{a} \sin\frac{n\pi y}{b} \sin\frac{p\pi z}{c} \hat{x} + \frac{n\pi}{b} \cos\frac{m\pi x}{a} \cos\frac{n\pi y}{b} \sin\frac{p\pi z}{c} \hat{y} + \frac{p\pi}{c} \cos\frac{m\pi x}{a} \sin\frac{n\pi y}{b} \cos\frac{p\pi z}{c} \hat{z} \qquad (6)$$

$\frac{d}{dR} f(R_{i,mnp})$ is obtained after some mathematical effort:

$$\frac{d}{dR} f(R) = -\frac{1}{R^2} \left\{ \frac{2}{\sqrt{\pi}} ER \, e^{-E^2 R^2} + \frac{\epsilon_r \pi^2}{E^2} + \Re \left[(1 + j2\pi\sqrt{\epsilon_r}R) e^{-j2\pi\sqrt{\epsilon_r}R} erfc(ER - j\frac{\pi\sqrt{\epsilon_r}}{E}) \right] \right\} \qquad (7)$$

Finally $\nabla R_{i,mnp}$ is expanded in the following form:

$$\nabla R_{i,mnp} = \frac{\partial X_i}{\partial x} \frac{X_i + 2ma}{R_{i,mnp}} \hat{x} + \frac{\partial Y_i}{\partial y} \frac{Y_i + 2nb}{R_{i,mnp}} \hat{y} + \frac{\partial Z_i}{\partial z} \frac{Z_i + 2pc}{R_{i,mnp}} \hat{z} \qquad (8)$$

in which $\frac{\partial X_i}{\partial x} = \pm 1$, $\frac{\partial Y_i}{\partial y} = \pm 1$, and $\frac{\partial Z_i}{\partial z} = \pm 1$.

B. Extraction of Singular Term

When the source and field points coincide, the Green's function becomes singular. For potential functions this singularity is of $\frac{1}{R}$ type similar to free space. To extract this singularity one can add and subtract a $\frac{1}{R}$ term so that $G = G_1 + (G_2 - \frac{1}{R_0}) + \frac{1}{R_0}$ in which $R_0 = \sqrt{(x-x')^2 + (y-y')^2 + (z-z')^2}$ and G represents any component of the potential Green's functions. Note that $\frac{1}{R_0}$ can be integrated analytically over the linear basis functions in MoM and the remaining part has a finite value at $R_0 \longrightarrow 0$ and the objective here is to calculate this finite value. It is evident from Eq. 1 that the only singular term appears in Eq. 1b when $m = n = p = i = 0$. If one separates this term the remaining series are all regular with finite value everywhere. After some mathematical manipulations, the following expression is obtained:

$$S_0 \triangleq \lim_{R_0 \to 0} \left(f(R_0) - \frac{1}{R_0} \right) = -2\pi\sqrt{\epsilon_r} \, Im\left\{ erfc\left(j\frac{\pi\sqrt{\epsilon_r}}{E} \right) \right\} - \frac{2E}{\sqrt{\pi}} e^{\frac{\epsilon_r \pi^2}{E^2}} \qquad (9)$$

in which $Im\,[erfc(j\sigma)] = -\frac{2}{\sqrt{\pi}} \int_0^\sigma e^{t^2} \, dt$. In fact, the Taylor series expansion of $f(R_0)$ around the origin is:

$$f(R_0) = S_0 + \frac{1}{R_0} + \sum_n \alpha_n R_0^n \qquad (10)$$

In Eq. 5 the only singular term corresponds to $m = n = p = i = 0$ in Eq. 5b and it is in the form of $\frac{1}{R_0^2}$. After some mathematical efforts the following expression is obtained for the Taylor series expansion of $\frac{d}{dR} f(R)$ around the origin:

$$\frac{d}{dR_0} f(R_0) = -2\epsilon_r \pi^2 + 0 - \frac{1}{R_0^2} + \sum_n \delta_n R_0^n \qquad (11)$$

or equivalently, $\lim_{R_0 \to 0} \left(\frac{d}{dR} f(R_0) + \frac{1}{R_0^2} \right) = -2\epsilon_r \pi^2$. Therefore, adding $\frac{\nabla R_0}{R_0^2}$ to Eq. 5b and subtracting $\frac{1}{R_0}$ from Eq. 1b lead to smooth functions that have finite value everywhere and can be integrated numerically over the basis functions while the integration of above singular terms is carried out analytically.

A. Complex Error Function

Complex error function is accurately evaluated through the algorithm presented in [3] but it is still quite time consuming. In this paper, a numerical quadrature on real axis is proposed to evaluate Eq. 2. $f(R)$ can be written in the following integral form:

$$f(R) = \frac{2}{\sqrt{\pi}} \int_E^\infty e^{-R^2 s^2 + \frac{\epsilon_r \pi^2}{4 s^2}} \, ds = \frac{2}{\sqrt{\pi}} \frac{1}{R} \int_0^\infty e^{-x^2} h(x) \, dx \tag{12}$$

in which $h(x) = exp\left(\frac{\epsilon_r \pi^2 R^2}{(x + R E)^2} - 2R E x - R^2 E^2\right)$. Special type of Gaussian quadratures presented in [4] can now be used to calculate $f(R)$ in Eq. 12. Weights and abscissae up to 15 order for this type of quadrature are tabulated in [4]. Intensive numerical experiments showed that this new approach is **two times faster** than using the complex error function directly. For distances very close to the source point one might still calculate the complex error function directly for higher accuracy.

B. Splitting Parameter E

This real parameter splits the computational burden between Eq. 1a and Eq. 1b. A near optimum value for this parameter in 3D case was presented in [5]. Numerical experiments reveal that there is a substantial loss of accuracy for cases where the true wavelength $\lambda = \lambda_o/\sqrt{\epsilon_r}$ becomes very small compared to the cavity dimensions. Careful examination of the terms in Eq. 1 shows that in these cases the exponential term in Eq. 1a can become a huge positive number for some combination of summation indices which results in a very large negative value for G_1 while a small value for E (obtained from [5]) or a large ϵ_r lead to a large imaginary part for the argument of the complementary error function in Eq. 1b which results in a very large positive value for G_2 and, subsequently, the subtraction of these two large numbers leads to a substantial error. The remedy for this problem is to increase the splitting parameter accordingly instead of using the optimum value. Here is a simple procedure proposed to calculate an appropriate value for E automatically:

1. Calculate E_{opt} from [5]

2. Calculate $U = \dfrac{\pi^2}{E_{opt}^2}\left(\epsilon_r - (\dfrac{1}{4a^2} + \dfrac{1}{4b^2} + \dfrac{1}{4c^2})\right)$

3. If $U < A$ then the value chosen for E is OK. A is an arbitrary positive constant which is chosen to be $A = 12$. Choice of A is arbitrary as long as e^A is not a very large number.

4. If $U > A$ then increase the value of E according to $E = E_{opt}\sqrt{\dfrac{U}{A}}$

The above procedure ensures that the value of E is always chosen appropriately so that the desired accuracy is achieved at small wavelengths. Note that the larger the value of E, the faster Eq. 1b converges and more terms will be needed in order for Eq. 1a to converge.

IV. NUMERICAL RESULTS

All the components of the scalar and vector potential Green's functions and the gradients of the vector potential functions for an arbitrary rectangular cavity filled with a material of dielectric constant ϵ_r have been implemented and tested numerically. Note that all the physical dimensions are normalized to λ_o for better numerical accuracy. As an example a cavity with dimensions $a = 0.5$, $b = 0.45$, and $c = 0.333$ filled with a material of $\epsilon_r = 1.0, 5.0, 40.0$ is considered. The source point is located at $x' = 0.25$, $y' = 0.28$, and $z' = 0.10$ while the observation point is chosen on a 2D grid of points at the same height as the source $z = z'$. Number of field points is equal to $51 \times 46 = 2346$. Singular terms are also extracted and only the remaining series are calculated. In Fig. 1 G_A^{xx} and G_F^{xx} components are plotted for the case in which the cavity is filled with a high dielectric constant material. Note that the singular term is going to be treated separately. In Fig. 2 the derivatives of G_A^{xx} which are needed in application of MPIE method to dielectric objects are plotted after extraction of singular terms. In this case the cavity is filled with a dielectric constant of $\epsilon_r = 5.0$. In Fig 3 the average number of terms required for each series in Eq. 1 to converge are listed for different components of potential Green's functions. In each cell the first row is the average number of terms needed in summation of Eq. 1a and the second row is the number of terms needed for Eq. 1b to converge. Convergence is achieved when the corresponding term in the series is less than 10^{-7}.

V. CONCLUSION

The Ewald method was applied to calculate the vector and scalar potential Green's function inside a uniformly filled rectangular cavity. The gradient of the components of vector potential Green's functions were also calculated. These derivatives are needed in application of the MPIE technique to shielded dielectric objects. Extraction of the singular terms in the Green's functions and expressions for the residue terms were also reported. Several numerical implementation issues were addressed leading to further enhancement of the computational speed and numerical stability.

REFERENCES

[1] K.E.Jordan, G.R.Richter, and P.Sheng, "An Efficient Numerical Evaluation of the Green's Function for the Helmholtz Operator on Periodic Structures," *J. Comp. Phys.*, vol. 63, pp. 222–235, 1986.
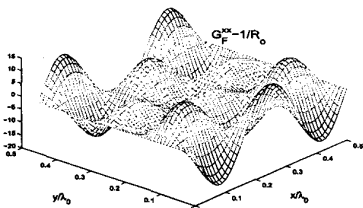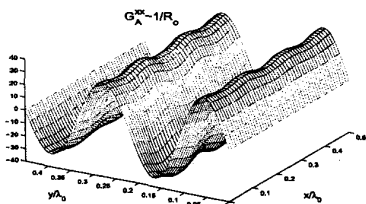
Fig. 1. $(G_A^{xx} - \frac{1}{R_0})$ and $(G_F^{xx} - \frac{1}{R_0})$ with $\epsilon_r = 40.0$
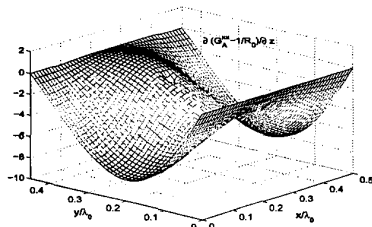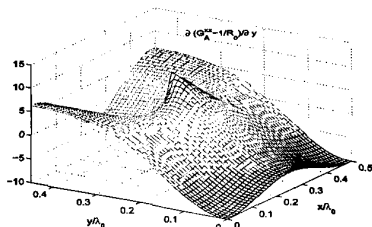

Fig. 2. $\frac{\partial}{\partial y}(G_A^{xx} - \frac{1}{R_0})$ and $\frac{\partial}{\partial z}(G_A^{xx} - \frac{1}{R_0})$ with $\epsilon_r = 5.0$

[2] M.J.Park, J.Park, and S.Nam, "Efficient Calculation of the Green's Function for the Rectangular Cavity," *IEEE Trans. Microwave Guided Wave Lett.*, vol. 8, no. 3, pp. 124–126, Mar. 1998.

[3] G.P.M.Poppe and C.M.J.Wijers, "More Efficient Computation of the Complex Error Function," *ACM Trans. Math. Soft.*, vol. 16, no. 1, pp. 38–46, Mar. 1990.

[4] N.M.Steen, G.D.Byrne, and E.M.Gelbard, "Gaussian Quadratures for the Integrals $\int_0^\infty \exp(-x^2)f(x)dx$ and $\int_0^b \exp(-x^2)f(x)dx$," *Mathematics of Computation*, vol. 23, no. 107, pp. 661–671, Jul. 1969.

[5] A.Kustepeli and A.Q.Martin, "On the Splitting Parameter in the Ewald Method," *IEEE Trans. Microwave Guided Wave Lett.*, vol. 10, no. 5, pp. 168–170, May 2000.

	$\epsilon_r = 1$	$\epsilon_r = 5$	$\epsilon_r = 40$
G_A^{xx}	45 46	53 55	223 58
G_F^{xx}	69 46	82 55	290 58
G_q^e	34 46	41 55	188 58

Fig. 3. Average number of terms needed for the convergence of each series in Eq. 1